

An Adaptable Robotic System for Assembling Irregular Earphone Parts on Factory Automation

Guiwei Zhang, Changle Li, Xuehe Zhang,
Gangfeng Liu, Yubin Liu, Jie Zhao and Shuo Xu.

*State Key Laboratory of Robotics and System
Harbin Institute of Technology
Harbin, China*

Abstract - The assembly of earphone parts in electro acoustic factory automation is a challenging problem for industrial robots. The main difficulties come from the fact that conventional industrial robots perform poorly on rapid-updated earphone parts, which are characterized by small size, variety and irregular shapes. What's worse, the robot cannot adapt to the earphone parts with different poses effectively. In order to tackle above problems, an adaptable robotic system guided by the 3D laser triangulation sensor and six-axis F/T sensor is built in this paper. In addition, to reduce position errors caused by the 3D sensor accidentally, an assembly strategy which is implemented by the admittance controller learned from human teaching, is proposed for assembling earphone parts. Specifically, AdaBoost-based GPR method is applied to derive the admittance gain, so that the controller perform effectively. A series of comparative experiments prove that the established system could demonstrate superior performance on the earphone parts with small size, variety and irregular shapes. Furthermore, it is also validated that the assembly strategy could be executed effectively on the earphone parts with different poses.

Index Terms – *laser-force guided robot system, assembling irregular parts, AdaBoost-based GPR admittance controller, learn from human teaching.*

I. INTRODUCTION

At present, the automated assembly of earphone parts in electroacoustic products industry is a challenging problem for industrial robots to execute [1]. As is well known, the earphone parts are characterized by small size, variety, fast upgrade speed and irregular shapes. Therefore, it is a crucial issue for robots to adapt to new earphone parts as quickly as possible on the premise that high assembly accuracy should be guaranteed. Furthermore, the robot is also required to perform effectively on the earphone parts with irregular shapes and uncertainties of poses.

In order to tackle above problems, a series of robot systems based on multi-sensor data fusion have been built in recent years. The robot system that combines 2D and 3D visual information was proposed by [2], to execute peg-in-hole assembling. However, since the system had no force feedback, it could not compensate for the position error from vision sensors. By contrast, the active compliance control system were introduced to eliminate uncertain position error effectively, and then to improve flexibility of assembly process in factory automation [3], [4], [5]. Two main implementations of active compliance control are impedance and admittance control [6]. In [7], an

impedance control scheme was used for geometrically complex parts assembling. Besides, the nested admittance controller for misaligned parts assembly tasks was established by [8].

Note that earphone parts on the assembly line are irregular, various and uncertain. Operators have to tune the impedance or admittance gain in the case of the parts with variety and uncertainties, so as to adapt to the different stiffness, damping or clearance of the contact conditions[9]. Obviously, the traditional tuning method of gains will result in poor effectiveness and adaptability. Therefore, the traditional active compliant control schemes cannot perform well on the housings with irregular shapes and uncertainties.

Conversely, human could execute the assembly task more effectively. If considering human inherent assembly skills as the controller, then its gains will be well tuned through learning from human demonstration [10],[11]. In [9], a vision-force guided robot system was established to collect “force/torque-velocity” data during human demonstration. Then the admittance gain was learned by Gaussian Mixture Regression [12]. Also inspired by human motion patterns, the guidance algorithm for complex parts assembling with the Gaussian mixture model, was developed by [11]. In [13], the deep reinforcement learning algorithm and an admittance controller coupled to the neural network was proposed for mixed deformable and rigid parts assembly tasks. Similarly, a recurrent neural network with reinforcement learning was trained by [14], to achieve assembling accurately.

However, most of the mentioned strategies based on learning from human demonstration require a significant amount of human demonstration and compute cost. Therefore, the schemes cannot adapt to rapid-updated earphones effectively, and thus cannot improve workplace efficiency.

In order to tackle above problems, an admittance controller that only requires a smaller number of human teaching and compute cost, is proposed in this paper. Compared with deriving the gain with Gaussian mixture regression [15], deep learning [16], neural networks [17], and random forests [18], etc. Gaussian process regression (GPR) can demonstrate higher prediction accuracy on the training dataset with low sample size ,high dimension and highly nonlinear relationships [19]. Furthermore, the most significant advantage of GPR with respect to support vector regression (SVR) is that it can produce truly probabilistic outputs with an explicit degree of prediction

uncertainty [20],[21]. In addition, there exist algorithms for GP hyperparameter optimization which the SVR framework lacks.

Statement of Contributions: The contributions of this paper are threefold. To begin with, a laser-force guided robot system is built for assembling irregular earphone parts on factory automation. In particular, the system performs well to the earphone parts with irregular shapes and variety. Furthermore, in order to reduce position error caused by 3D laser sensor accidentally, a novel assembly strategy is proposed. Specifically, the strategy is implemented by an admittance controller learned from human teaching, and is able to be executed effectively on the earphone parts with different poses. Furthermore, the AdaBoost-based GPR method is applied to obtain the admittance gain. The most advantage of the method is that it can show superior performance and excellent generalization for unseen data in the case of a small amount of training data.

Organization: The remainder of this paper is organized as follows. Section II presents the configuration of laser-force guided robot system. Section III describes functional requirements and assembly process on the industrial assembly line. Section IV shows the assembly strategy implemented by the admittance controller based on learning from human teaching, and elaborates how to apply AdaBoost-based GPR method to derive the admittance gain. Section V conducts a series of comparative experiments and then provides the experimental evaluations. Section VI summarizes the results and indicates directions for future work.

II. CONFIGURATION OF THE ROBOT SYSTEM

As shown in Fig. 1, the collaborative industrial robot UR5, guided by the 3D laser triangulation sensor and six-axis F/T sensor is utilized in automation assembly line. Specifically, the UR5 robot with six degrees of freedom are highly repeatable, of which its repeatability can reach ± 0.1 mm. Furthermore, the 3D laser sensor mounted on a ball screw, is driven by a servo motor for linear motion. Besides, the F/T sensor fixed between the gripper and the robot is used to measure the force and torques applied at the gripper. The details of the 3D laser sensor and F/T sensor are described as below.

A. 3D Laser Triangulation Sensor

The 3D laser sensor C5-2040CS23-100 which is made from AT-Automation Technology GmbH in Germany, is applied in the system. It is optimized for 3D profile measurement by means of laser triangulation technique, and then the 3D profile extraction is performed by using high performance Field Programmable Gate Array processors. At the same time the 3D profile data is sent to the PC over a Gigabit Ethernet interface (GigE).

As seen in Fig. 2, the model overview of the 3D laser triangulation sensor is demonstrated, while Table I illustrates the detailed measurement specifications of the 3D laser sensor. It can be seen that reasonable measurement height of the sensor range from 86—126 mm, while the field of view from 90—110 mm.

B. Six-axis F/T sensor

ATI-Gamma F/T sensor is used, of which the maximum allowable overload values are 6.9 to 31.6 times rated capacities.

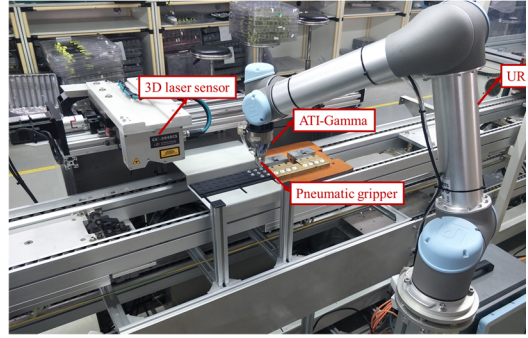


Fig. 1: Configuration of the robot system

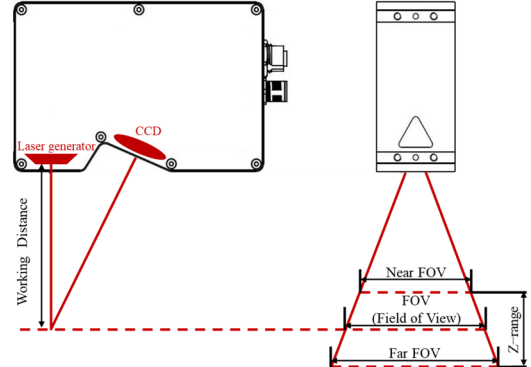


Fig. 2: Model overview of the 3D laser triangulation sensor

TABLE I
MEASUREMENT SPECIFICATIONS OF THE 3D LASER SENSOR

Model Name	C5-2040CS23-100
Resolution(X) [mm/pixel]	0.049
Resolution(Z) [mm/pixel]	0.00189
Nominal FOV [mm]	100
Z-range [mm]	40
Working Distance [mm]	106

TABLE II
SPECIFICATIONS OF ATI-GAMMA F/T SENSOR

Model Name	SI-130-10
Sensing ranges	Fx, Fy 130 N Fz 400 N Tx,Ty 10 Nm Tz 10 Nm
Resolution	Fx, Fy 1/40 N Fz 1/20 N Tx,Ty 1/800 Nm Tz 1/800 Nm

In addition, forces and torques applied on the sensor can be simultaneously measured by the Network Force/Torque (Net F/T) sensor system. The Net F/T communicates with PC via EtherNet/IP, CAN Bus, Ethernet, and is compatible with DeviceNet. Detailed specifications of the F/T sensor are listed in Table II.



Fig. 3: Assembly requirements for irregular earphone parts

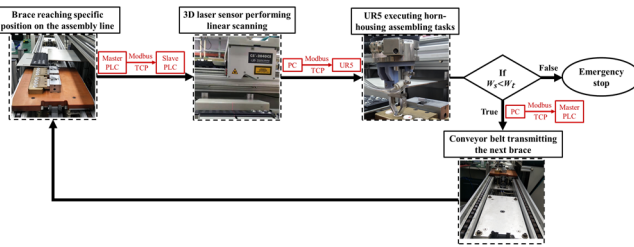


Fig. 4: Diagram of assembly process on the factory assembly line

III. FUNCTIONAL ANALYSIS OF THE PROPOSED SYSTEM

A. Function requirements

In order to meet function requirements for assembling earphone parts on factory automation, the system has to meet the following characteristics.

1) *Rapid Assembling Speed*: In factory automation, earphone parts are characterized by fast update speed and large production volume. To improve efficiency, the robot is required to complete horn-housing assembly every three seconds.

2) *Superior Adaptability to Irregular Earphone Parts*: The main difficulties of assembling earphone parts come from the fact that the parts are characterized by small size and irregular shapes. Specifically, there is irregular dispensing on the surface of the earphone horn. Therefore, the robot should perform well to the earphone parts with irregular shapes. Particularly on the industrial assembly line, the robot is required to make the dispensing be towards the left side of the housing fixed in the brace. Similarly for the right housing, the dispensing should be towards the right side, as demonstrated in Fig. 3.

3) *Protecting weak stiffness materials*: Earphone parts are machined from weak stiffness materials. Thus, the robot must be stopped urgently when the end gripper is extremely stressed to avoid damage to parts with weak stiffness materials.

B. Assembly Process on Factory Assembly Line

As shown in Fig. 4, the specific steps of the robot system to perform assembling task can be divided as follow.

- When the brace with earphone housings reaches the specific position on the assembly line, the master PLC communicates with the slave PLC via Modbus TCP protocol. Then the slave PLC starts the servo motor to drive the 3D laser for linear scanning.
- After the 3D laser sensor finishes scanning, the captured vision image will be processed on the PC. Then, the

poses of earphone parts in the robot coordinate frame will be accurately obtained.

- Subsequently, the solved poses of earphone parts will be sent to the UR5 robot via Modbus TCP protocol. Afterwards, assembling tasks can be executed by the UR5 robot effectively. Note that if forces and torques applied on the end-gripper exceeds the threshold during assembly, the robot will be stopped urgently to avoid damage to earphone parts with weak stiffness materials. For description simplicity, the wrench is used to denote both forces and torques applied on the end-gripper $W = [F_x, F_y, F_z, T_x, T_y, T_z]$

IV. ASSEMBLY STRATEGY GUIDED BY ADMITTANCE CONTROLLER BASED ON LEARNING FROM HUMAN TEACHING

A. Assembly Strategy Guided by Admittance Controller

To reduce position error caused by 3D laser sensor accidentally, a novel assembly strategy is proposed. In particular, the strategy is implemented by an admittance controller based on learning from human teaching.

As demonstrated in Fig. 5, the strategy consists of six phases. In phase (I), the earphone horn approaches the housing vertically, until there are contact wrench sensed by F/T sensor. If the wrench is not consistent with the desired for proper assembling, position error can be proved. Then in phase (II), the horn is rotated θ angle around its z-axis, to make its x-axis parallel to $\overrightarrow{OO'}$. In phase (III) the horn is rotated slight δ angle around its y-axis, so that lower edge of the hole inside the housing. In phase (IV) the horn moves along its -x-axis until a contact force sensed when it reaches the inside face of the housing. By doing so, the horn is completely inside the housing. The phase (V) is to make center line of the horn parallel to that of the housing .Finally in phase (VI) ,the insertion is completed by pushing the horn into the housing along -z-axis until sensed wrench exceeds the limit.

Note that the most important phase above is to solve θ in phase (II). Then, the horn will be rotated θ angle around its z-axis, which will be denoted as the corrective pose $x_c = [0, 0, 0, 0, 0, \theta]$. To derive x_c , the horn will be tilted slightly around its axes, so that it is in point contact with the housing, as shown in Fig. 5 (a) and (b) . Hence the relationship between θ and contact points $P(p_x, p_y)$ and $P'(p'_x, p'_y)$ are as below.

$$\overrightarrow{OP} + \overrightarrow{OP'} = \gamma \overrightarrow{OO'} \quad (1)$$

$$\theta = \pi - \arccos[(\overrightarrow{OP} + \overrightarrow{OP'}) \cdot \vec{e} / |\overrightarrow{OP} + \overrightarrow{OP'}|] \quad (2)$$

Where γ is a constant ,while \vec{e} is the unit vector of the x-axis direction in the sensor frame $\{S\}$ and the operator $|\cdot|$ denote the module of the vector.

According to the force and torque balance, the coordinates of P in Fig. 5 (a) are related to sensed wrench at the moment, similarly for P' . Thus, \overrightarrow{OP} and $\overrightarrow{OP'}$ can be denoted as

$$f: W \rightarrow \overrightarrow{OP}, \overrightarrow{OP'} \quad (3)$$

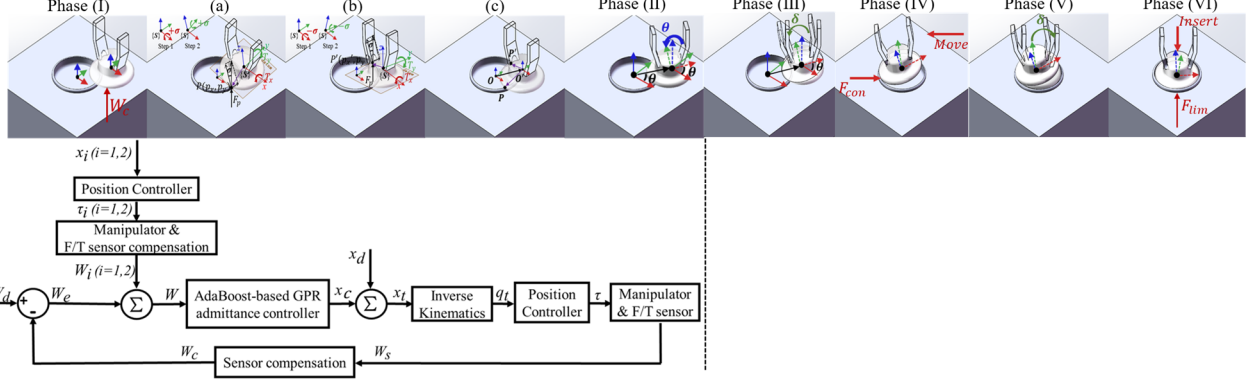


Fig. 5: Block diagram of earphone parts assembly strategy implemented by the admittance controller learned from human teaching

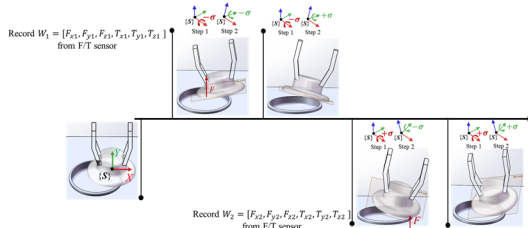


Fig. 6: Schematic diagram of collecting the training data $\{(W'_i, \theta'_i)\}_{i=1}^n$ at one of contact points

To obtain the corrective pose x_c effectively, an admittance controller learned from human teaching is established. As illustrated in Fig. 5, x_i ($i=1,2$) are poses of the horn, which are also poses of TCP of UR5. Besides, τ_i and W_i ($i=1,2$) are the corresponding torque and sensed wrench. Note that the combination of W_1 , W_2 and W_e is utilized to determine x_c , then the horn will be guided to the target pose x_t , as shown in Phase (II). Once the target pose is reached accurately by the admittance controller, following phases will be achieved successfully with less error. Other meanings of the symbols shown in Fig. 5 are as follow: x_d denotes the desired pose from 3D laser sensor in Cartesian space, x_c and x_t are corrective pose and target pose. Besides, W_d , W_s and W_c are desired, sensed and contact wrench respectively. The variables q_t and q_r are target and robot positions in joint space, which is solved by inverse kinematics.

Different from traditional tuning method of the admittance gain, the admittance controller learned from human teaching is to collect training data $\{(W'_i, \theta'_i)\}_{i=1}^n$ during human teaching, then a proper admittance gain can be regressed by the dataset. Therefore, Once the unseen wrench is input into the admittance controller, the admittance gain will be utilized to predict the corresponding x_c . Specific details about the collection of $\{(W'_i, \theta'_i)\}_{i=1}^n$ will be shown below.

B. Data Acquisition and Processing

With the help of the 3D laser sensor, 45 contact points on the circumference of the housing with 8° angle between each point can be sampled. Then, the robot is taught to make the end-gripper which has gripped the horn reach each point, respectively.

For one of the contact points as illustrated in Fig. 6, the coordinate frame of the F/T sensor $\{S\}$ is located at the center of the horn, which can be also regarded as the frame of the horn. The horn will be rotated around its own $\pm x$ axis and $\pm y$ axis, so that it is in point contact with the housing. If the horn is in point contact with the housing, the F/T sensor could detect $W_i = [F_{xi}, F_{yi}, F_{zi}, T_{xi}, T_{yi}, T_{zi}]$ ($i=1,2$). Otherwise, the F/T sensor could only detect interference which can be ignored.

C. Learn Admittance Gain with AdaBoost-based GPR method

In terms of the regression model in the admittance controller

$$\theta = f(W) + \varepsilon \quad (4)$$

where we assume that $f(W) \sim GP(\mu, k)$, $\varepsilon \sim N(0, \sigma_n^2)$. Given training data $\{(W'_i, \theta'_i)\}_{i=1}^n$ during human teaching, Gaussian process regression model is used to derive the joint distribution of observed $\vec{\theta}' = [\theta'_1, \theta'_2, \dots, \theta'_n]$ and predict θ_* for unseen input W , as seen in (6).

$$[\vec{\theta}_*] \sim N \left(\begin{bmatrix} \mu(\vec{W}') \\ \mu(W) \end{bmatrix}, \begin{bmatrix} K(\vec{W}', \vec{W}') + \sigma_n^2 I & K(W, \vec{W}')^T \\ K(W, \vec{W}') & K(W, W) \end{bmatrix} \right) \quad (5)$$

Usually for notational simplicity, the mean function $\mu(\cdot)$ will be taken to zero [22]. Besides, $K(\vec{W}', \vec{W}')$ is the $n \times n$ covariance matrix of which the (i,j) -th element $K_{ij} = k(x_i, x_j)$, and similarly for the other matrixes $K(W, \vec{W}')$ and $K(W, W)$. Then, with the marginalization and conditional distribution theory in [23], the key predictive distribution can be derived by

$$p(\theta_* | \vec{W}', \vec{\theta}, W) \sim N(\hat{\mu}, \hat{\Sigma}) \quad (6)$$

$$\hat{\mu} = K(W, \vec{W}')^T (K(\vec{W}', \vec{W}') + \sigma_n^2 I)^{-1} \vec{\theta}' \quad (7)$$

$$\hat{\Sigma} = K(W, W) - K(W, \vec{W}')^T (K(\vec{W}', \vec{W}') + \sigma_n^2 I)^{-1} K(W, \vec{W}') \quad (8)$$

As can be seen that kernel function $k(\cdot, \cdot)$ plays a crucial role in the predictive mean and variance. Although Squared

Exponential kernel function is widely-used due to its high smoothness[24],[25], it is overly smooth and unrealistic for modeling certain physical processes. Thus, Matern covariance function is recommended [26].

$$K(W, W') = \sigma^2(1 + \sqrt{3}\|W - W'\|/l)exp(-\sqrt{3}\|W - W'\|/l) \quad (9)$$

Where $\|\cdot\|$ is Euclidean norm, parameters σ and l are hyper-parameters optimized by maximizing log marginal likelihood function [22] , which is denoted as φ in this paper.

To execute assembly tasks effectively for rapid-updated earphone parts, training data $\{(W'_i, \theta'_i)\}_{i=1}^n$ input into the admittance controller should be as small as possible. However, training data that are too small increase the likelihood of overfitting [27]. In order to improve the generalization ability, AdaBoost algorithm is applied to ensemble GPR method[28], [29]. The basic idea is to train a weak GPR model with a different distribution of training data iteratively, then the output of each weak GPR model is combined as the final output. Specifically, if GPR model has a larger error on a training sample, then the weight of the sample will increase in the next iteration [30]. The algorithm detail is listed in Algorithm 1.

Fig. 7 illustrates the admittance block formulated by the AdaBoost-based GPR model. Substituting (7) into $y_{final}(W)$ defined in Algorithm 1, we can predict how large the final θ is for W input into the admittance block by

$$\theta = \sum_{t=1}^T \alpha_t K_t(W, \bar{W})^T / \sum_{t=1}^T \log(\beta_t) \quad (10)$$

$$\alpha_t = \log(\beta_t)(K_t(\bar{W}, \bar{W}) + \sigma_n^2 I)^{-1} \bar{\theta}' \quad (11)$$

Thus, it can be considered that AdaBoost-based admittance block is composed of T linear dampers, where each damper has a unique admittance $K_t(W, \bar{W})^T$ ($t=1, 2, \dots, n$), respectively. In addition, each damper has a nonlinear weight α_t denoting its contribution to the whole block. The output of the admittance block is generated by the weighted sum of T dampers' outputs.

V. EXPERIMENTS

A. Image Processing for Irregular Earphone Parts

As shown in Fig. 8, the 3D surface-based matching algorithm with MVTec HALCON is applied to derive 3D poses of earphone parts in the sensor coordinate frame. It can be seen that the housings with various poses (Pose 0, Pose 1, Pose 2) can be recognized accurately. Furthermore, the 3D laser sensor performs well to the earphone parts with irregular dispensing. Specifically, 3D pose of the dispensing on the horn is identified effectively. Thus, it is validated that the 3D laser triangulation sensor can demonstrate superior performance on the earphone parts with different poses and irregular shapes.

B. Validation and Comparison

In this section, two questions should be answered:

- 1) Can the proposed strategy be executed successfully on the earphone housings with different 3D poses?

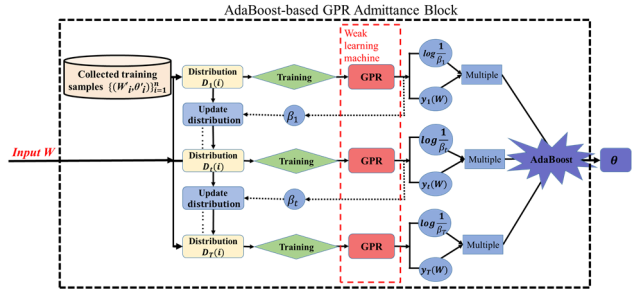


Fig. 7: Block diagram of the AdaBoost-based GPR admittance controller

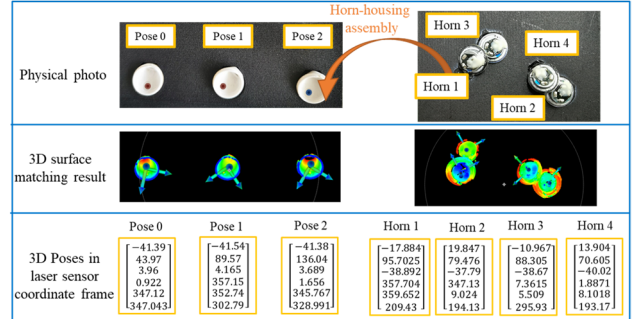


Fig. 8: Surface-based 3D matching results with MVTec HALCON.

Algorithm 1: AdaBoost-based GPR

Input:

- 1: Collected training samples, $\{(W_i, \theta_i)\}_{i=1}^n$
- 2: Weak learning machine (GPR)
- 3: Integer T specifying number of weak learner
- 4: Threshold φ for demarcating correct and incorrect predictions

Initialize:

- 5: Machine number or iteration $t=1$

- 6: Distribution $D_t(i) = 1/n$ for all i

- 7: Error rate ε_t

Iterate:

- 8: While($t \leq T$):

- 9: Provide $\{W_i\}_{i=1}^n$ with distribution D_t

- 10: Predict the value $y_t(W_*)$ with GPR model

- 11: Calculate the error rate of $y_t(W_*)$

$$\varepsilon_t = \sum_{i: |y_t(W_i) - \theta_i| > \varphi} D_t(i)$$

- 12: Set $\beta_t = 1/\varepsilon_t^2$

- 13: Update distribution D_t as

$$D_{t+1}(i) = \frac{D_t(i)}{Z_t} \times \begin{cases} \beta_t, & |y_t(W_i) - \theta_i| > \varphi \\ 1, & otherwise \end{cases}$$

Where Z_t is a normalization factor chosen such that D_{t+1} will be a distribution.

- 14: $t=t+1$

Output the final prediction

$$15: y_{final}(W_*) = \sum_{t=1}^T \log(\beta_t) y_t(W_*) / \sum_{t=1}^T \log(\beta_t)$$

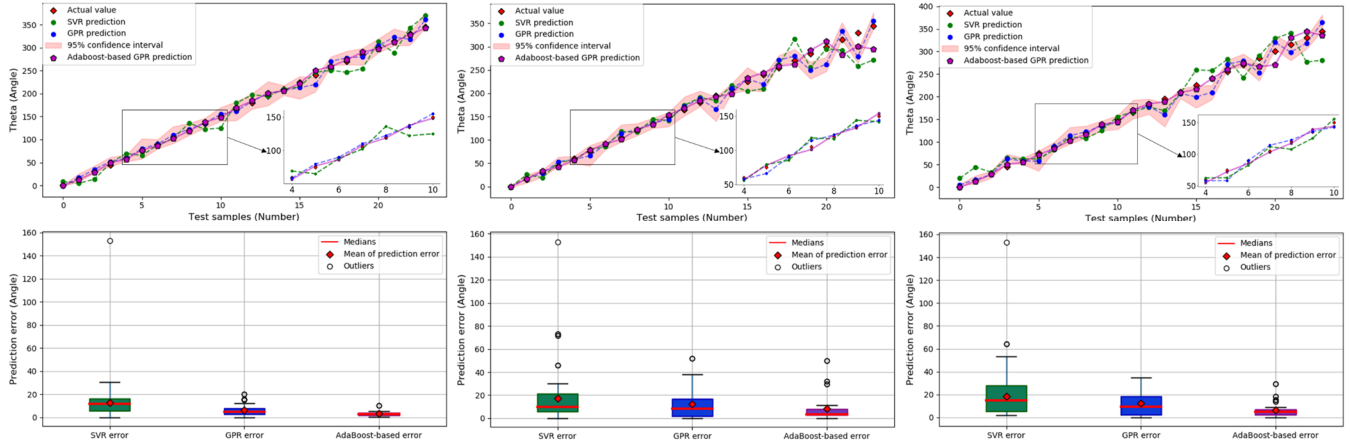


Fig. 9: Comparing prediction results of each method on the housings with different poses, from left to right: Pose 0, Pose 1, Pose 2. Top: Comparison of prediction curves. Bottom: Comparison of prediction error. Note that the training dataset $\{(W_i, \theta'_i)\}_{i=1}^n$ is only collected at contact points on the circumference of the housing in Pose 0, with 8° angle between each point. Then the dataset is used to train SVR, GPR, AdaBoost-based GPR method respectively. Subsequently, the trained methods are used to predict how large θ should be for unseen W measured at points on the circumference of housings in Pose 0, Pose 1 and Pose 2, with 15° between each point.

2) Does the developed AdaBoost-based GPR admittance controller demonstrate higher prediciton accuracy and more excellent generalization in the case of small training samples?

To answer the first question, training data $\{(W'_i, \theta'_i)\}_{i=1}^n$ is collected manually at points on the circumference of the housing in *Pose 0*, with 8° angle between each point. Then the dataset is trained to obtain the gain of the AdaBoost-based GPR admittance controller. In order to validate the adaptability of the controller, the trained method is used to predict how large θ should be for unseen wrench W measured at points on the circumference of housings in *Pose 0*, *Pose 1* and *Pose 2*, with 15° between each point.. Finally, the deviation of prediction value and real value is utilized to evaluate the strategy quantitatively. For the second question, the support vector regression method is utilized as the compared method to validate the generalization of the AdaBoost-based GPR admittance controller.

C. Results

Fig. 9 illustrates the prediction results of each method on the housings with different poses. TABLE I demonstrate the root mean square error (RMSE) of prediction results for each method. Note that the numbers in parentheses indicate the RMSE after outliers are removed. From above results, the following observations can be drawn.

- Both SVR and GPR show poor performance for unseen wrench . In particular, the SVR method with RBF kernel shows worse prediction accuracy. This validates that the RBF kernel is overly smooth and indeed unrealistic for modeling certain physical processes. Besides, the GPR method cannot demonstrate good generalization ability using hyperparameters with maximum of marginal likelihood, as can be seen in Fig. 10. By contrast, AdaBoost-based GPR could generalize better from training data to unseen data. It is confirmed that it can improve generalization of GPR method for housings with different poses.

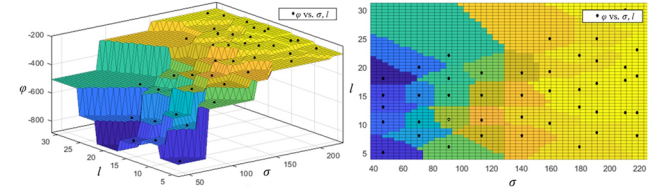


Fig. 10: Distribution of the log marginal likelihood on the hyperparameters of Matern kernel

TABLE III
RMSE COMPARISON(UNIT: ANGLE)

	<i>AdaBoost-based GPR</i>	<i>GPR</i>	<i>SVR</i>
Pose 0	3.0114	8.0750	15.1796
Pose 1	14.4250(3.2766)	18.1427(10.4034)	26.1999(17.4922)
Pose 2	9.3592(4.0716)	16.0454(13.6370)	24.5556(18.8214)

- For the housings with different poses, AdaBoost-based GPR performs well only with fewer training samples. Thus, it can be inferred that the assembly strategy implemented by AdaBoost-based GPR admittance controller, could adapt to the housings with uncertainties of poses effectively.
- However, AdaBoost-based GPR perform poorly at some contact points. The main reason may be that the horn is not in point contact with the housing when sensed wrench is recorded. Also, the interference due to environmental interactions may be another cause. This indicates that although AdaBoost-based GPR can be less susceptible to the overfitting problem, it can be sensitive to noisy data and outliers especially.

VI. CONCLUSIONS

Conclusion: In this paper, a laser-force guided robot system is built for assembling earphone parts on factory automation. The most significant advantage of the system is that it performs well to irregular parts with small size and variety. To reduce position errors accidentally from the 3D sensor, an assembly

strategy is proposed for assembling earphone parts with different poses. In particular, the strategy is implemented by the admittance controller learned from human teaching. Furthermore, AdaBoost-based GPR method is applied to obtain the admittance gain, so that the controller can demonstrate superior prediction performance with fewer training samples. Verification experiments are conducted to prove that the robot system could perform well to irregular earphone parts with small size and various poses on factory automation. Furthermore, comparative experiments have validated that the strategy implemented by AdaBoost-based GPR admittance controller could show superior performance on parts with different poses

Future work: How to guarantee the system stability will be one promising extension for future work. It is crucial to analyse the stability conditions of closed-loop system. Besides, more effective methods should be proposed to collect training samples, to help the robot perform better for unseen data.

ACKNOWLEDGMENT

This work is supported by the National Natural Science Foundation of China (NSFC) (Grant no. U1713202, 61803126), National High-tech R&D Program of China (No. 2017YFB1303600) and DongGuan Major Special Project(no. 201721502011).

REFERENCES

- [1] A. Y. C. Nee, *Handbook of Manufacturing Engineering and Technology*. 2014.
- [2] D. T. Le, M. Andulkar, W. Zou, J. P. Stadler, and U. Berger, "Self adaptive system for flexible robot assembly operation," in *IEEE International Conference on Emerging Technologies & Factory Automation*, 2016.
- [3] F. Chen, F. Cannella, J. Huang, H. Sasaki, and T. Fukuda, "A study on error recovery search strategies of electronic connector mating for robotic fault-tolerant assembly," *Journal of Intelligent & Robotic Systems*, vol. 81, no. 2, pp. 257-271, 2016.
- [4] J. Takahashi, T. Fukukawa, and T. Fukuda, "Passive alignment principle for robotic assembly between a ring and a shaft with extremely narrow clearance," *IEEE/ASME Transactions on Mechatronics*, vol. 21, no. 1, pp. 196-204, 2015.
- [5] J. Huang, Y. Wang, and T. Fukuda, "Set-membership-based fault detection and isolation for robotic assembly of electrical connectors," *IEEE Transactions on Automation Science and Engineering*, vol. 15, no. 1, pp. 160-171, 2016.
- [6] A. Calanca, R. Muradore, and P. Fiorini, "A review of algorithms for compliant control of stiff and fixed-compliance robots," *IEEE/ASME Transactions on Mechatronics*, vol. 21, no. 2, pp. 613-624, 2015.
- [7] H.-C. Song, Y.-L. Kim, and J.-B. Song, "Automated guidance of peg-in-hole assembly tasks for complex-shaped parts," in *2014 IEEE/RSJ International Conference on Intelligent Robots and Systems*, 2014, pp. 4517-4522: IEEE.
- [8] N. Mol, J. Smisek, R. Babuška, and A. Schiele, "Nested compliant admittance control for robotic mechanical assembly of misaligned and tightly tolerated parts," in *2016 IEEE International Conference on Systems, Man, and Cybernetics (SMC)*, 2016, pp. 002717-002722: IEEE.
- [9] T. Tang, H.-C. Lin, Y. Zhao, Y. Fan, W. Chen, and M. Tomizuka, "Teach industrial robots peg-hole-insertion by human demonstration," in *2016 IEEE International Conference on Advanced Intelligent Mechatronics (AIM)*, 2016, pp. 488-494: IEEE.
- [10]M. W. Abdullah, H. Roth, M. Weyrich, and J. Wahrburg, "An approach for peg-in-hole assembling using intuitive search algorithm based on human behavior and carried by sensors guided industrial robot," *IFAC-PapersOnLine*, vol. 48, no. 3, pp. 1476-1481, 2015.
- [11]H.-C. Song, Y.-L. Kim, and J.-B. Song, "Guidance algorithm for complex-shape peg-in-hole strategy based on geometrical information and force control," *Advanced Robotics*, vol. 30, no. 8, pp. 552-563, 2016.
- [12]H. G. Sung, "Gaussian mixture regression and classification," Rice University, 2004.
- [13]J. Luo, E. Solowjow, C. Wen, J. A. Ojea, and A. M. Agogino, "Deep reinforcement learning for robotic assembly of mixed deformable and rigid objects," in *2018 IEEE/RSJ International Conference on Intelligent Robots and Systems (IROS)*, 2018, pp. 2062-2069: IEEE.
- [14]T. Inoue, G. De Magistris, A. Munawar, T. Yokoya, and R. Tachibana, "Deep reinforcement learning for high precision assembly tasks," in *2017 IEEE/RSJ International Conference on Intelligent Robots and Systems (IROS)*, 2017, pp. 819-825: IEEE.
- [15]A. Lagrange, M. Faubel, and M. Grizonnet, "Large-scale feature selection with Gaussian mixture models for the classification of high dimensional remote sensing images," *IEEE Transactions on Computational Imaging*, vol. 3, no. 2, pp. 230-242, 2017.
- [16]Q. Wang, J. Wan, and Y. Yuan, "Deep metric learning for crowdedness regression," *IEEE Transactions on Circuits and Systems for Video Technology*, vol. 28, no. 10, pp. 2633-2643, 2017.
- [17]A. Roy and S. Todorovic, "Monocular depth estimation using neural regression forest," in *Proceedings of the IEEE Conference on Computer Vision and Pattern Recognition*, 2016, pp. 5506-5514.
- [18]Y. Gao, Y. Shao, J. Lian, A. Z. Wang, R. C. Chen, and D. Shen, "Accurate segmentation of CT male pelvic organs via regression-based deformable models and multi-task random forests," *IEEE transactions on medical imaging*, vol. 35, no. 6, pp. 1532-1543, 2016.
- [19]X. Fan, Y. Wang, X. Tang, R. Gao, and Z. Luo, "Two-layer Gaussian process regression with example selection for image dehazing," *IEEE Transactions on Circuits and Systems for Video Technology*, vol. 27, no. 12, pp. 2505-2517, 2016.
- [20]M. Awad and R. Khanna, "Support Vector Regression," in *Efficient Learning Machines: Theories, Concepts, and Applications for Engineers and System Designers* Berkeley, CA: Apress, 2015, pp. 67-80.
- [21]K. Markov and T. Matsui, "Music genre and emotion recognition using Gaussian processes," *IEEE access*, vol. 2, pp. 688-697, 2014.
- [22]C. Rasmussen and C. Williams, "Gaussian process for machine learning," ed: the MIT Press, 2005.
- [23]I. A. Ibragimov and Y. A. e. Rozanov, *Gaussian random processes*. Springer Science & Business Media, 2012.
- [24]S. Roberts, M. Osborne, M. Ebden, S. Reece, N. Gibson, and S. Aigrain, "Gaussian processes for time-series modelling," *Philosophical Transactions of the Royal Society A: Mathematical, Physical and Engineering Sciences*, vol. 371, no. 1984, p. 20110550, 2013.
- [25]C. K. Williams and C. E. Rasmussen, *Gaussian processes for machine learning* (no. 3). MIT press Cambridge, MA, 2006.
- [26]W. Sun, M. Xue, H. Yu, H. Tang, and A. Lin, "Augmentation of Fingerprints for Indoor WiFi Localization Based on Gaussian Process Regression," *IEEE Transactions on Vehicular Technology*, vol. 67, no. 11, pp. 10896-10905, 2018.
- [27]P. M. Domingos, "A few useful things to know about machine learning," *Commun. acm*, vol. 55, no. 10, pp. 78-87, 2012.
- [28]D. P. Solomatine and D. L. Shrestha, "AdaBoost. RT: a boosting algorithm for regression problems," in *2004 IEEE International Joint Conference on Neural Networks (IEEE Cat. No. 04CH37541)*, 2004, vol. 2, pp. 1163-1168: IEEE.
- [29]Q. Huang, Y. Chen, L. Liu, D. Tao, and X. Li, "On combining biclustering mining and AdaBoost for breast tumor classification," *IEEE Transactions on Knowledge and Data Engineering*, 2019.
- [30]H.-X. Tian and Z.-Z. Mao, "An ensemble ELM based on modified AdaBoost. RT algorithm for predicting the temperature of molten steel in ladle furnace," *IEEE Transactions on Automation Science and Engineering*, vol. 7, no. 1, pp. 73-80, 2009.